Annals of Glaciology 37 2003

Ice-fabrics study in the upper 1500 m of the Dome C (East Antarctica) deep ice core

Yun WANG,[1] Sepp KIPFSTUHL,[1] Nobuhiko AZUMA,[2] Thorsteinn THORSTEINSSON,[1,3] Heinz MILLER[1]

[1] *Alfred Wegener Institute for Polar and Marine Research, P.O. Box 120161, D-27515 Bremerhaven, Germany*
E-mail: ywang@awi-bremerhaven.de

[2] *Department of Mechanical Engineering, Nagaoka University of Technology, Kamitomioka cho 1603-1, Nagaoka 940-2188, Japan*

[3] *Department of Geophysics, Science Institute, University of Iceland, Dunhaga 3, IS-107 Reykjavík, Iceland*

ABSTRACT. A study of *c*-axis orientations in the upper 1500 m of the Dome C (East Antarctica) deep ice core has been carried out using an automatic ice-fabric analyzer (AIFA). Twenty-nine vertical and a few horizontal thin sections from different depths in the core have been analyzed. Several statistical parameters describing fabric strength and fabric shapes have been calculated from the *c*-axis orientation data. The fabric diagrams display a near-random *c*-axis orientation distribution in the uppermost parts of the ice sheet. A tendency of *c*-axis rotation towards a broad single-maximum fabric is observed in the lowest part of the studied interval. The fabric development at Dome C thus appears typical for ice-sheet summit and dome sites. The fabric development at Dome C is compared with the fabric evolution in the Dome F and GRIP ice cores, and data on crystal size obtained with image-analysis techniques are presented. Studies of misorientation angles between the *c* axes of neighbouring crystals reveal little evidence for polygonization, but microscopic observations show that sub-grain boundaries are present in half of the grains at any depth.

INTRODUCTION

Fabrics provide a record of deformation history and control the viscosity of ice during further deformation (e.g. Alley, 1988; Azuma, 1994). Fabric (*c*-axis orientation distribution) and texture (crystal size/shape) studies have been carried out on artificial and natural glacier ice deformed in the laboratory (e.g. Jacka and Maccagnan, 1984; Azuma and Higashi, 1985; Pimienta and others, 1987; Shoji and Langway, 1988). Based on these observations, basal plane glide has been accepted as the main mechanism of ice deformation. Ice-fabric patterns characteristic for simple stress configurations in polar ice sheets have been observed in polar ice sheets. In the absence of recrystallization, rotation of the the basal planes and the *c* axis during deformation by basal glide leads to the formation of a single-maximum fabric under uniaxial compression or simple shear (Alley, 1992; Thorsteinsson and others, 1997; Azuma and others, 1999); to a girdle type under uniaxial tension (Fujita and others, 1987; Lipenkov and others, 1989); and to an elongated single maximum under pure shear (Wang and others, 2002). For ice sheets where the stress pattern is determined by the surface and bedrock topographies, the type of fabric pattern observed at a particular location can be predicted. Dome C is situated on a local dome in East Antarctica, where uniaxial vertical compression is expected to be the dominant stress pattern. Consequently, a single-maximum fabric is expected to evolve with depth. In this paper, we present fabric results from the Dome C core, obtained with an automatic ice-fabric analyzer (AIFA) which has previously been used to measure fabrics in the Dome Fuji (Dome F) and North Greenland Ice-core Project (NorthGRIP) deep ice cores. In order to assess the occurrence of polygonization, a study of misorientation angles between the *c* axes of neighbouring crystals has been carried out on the dataset, using the method of Alley and others (1995). The results from this study are compared with information derived from microscopic studies of sub-grain boundaries. Results from crystal-size measurements carried out using image-analysis techniques are presented, and data on fabric development at Dome C are compared with similar data from the GRIP and Dome F deep ice cores.

SAMPLING AND METHODS

Within the framework of the European Project for Ice Coring in Antarctica (EPICA), a deep ice core is being drilled at Dome C. Deep drilling was initiated during the 1996/97 season at 75°06′ S, 123°12′ E (3233 m a.s.l.). The drill became stuck at 780 m depth during the 1998/99 season, and drilling was restarted during austral summer 1999/2000. At the end of the 2001/02 season, drilling had reached the present depth of 2871 m. For this study, samples from the first core are used down to 575 m depth. The thin sections from the first core, both vertical and horizontal, were prepared in the field using standard methods. The surface was covered with silicone oil, and the sections were then wrapped with fresh film and packed in plastic bags. During the 2000/01 season, vertical thin sections were made from 1 cm thick, 6 cm wide sections cut from the side of the second core, in the depth interval 654–1451 m. In total, 33 samples were made at intervals varying between 12 and 150 m. After transport to Europe, the samples were stored at temperatures below −25°C. The meas-

https://doi.org/10.3189/172756403781816031 Published online by Cambridge University Press

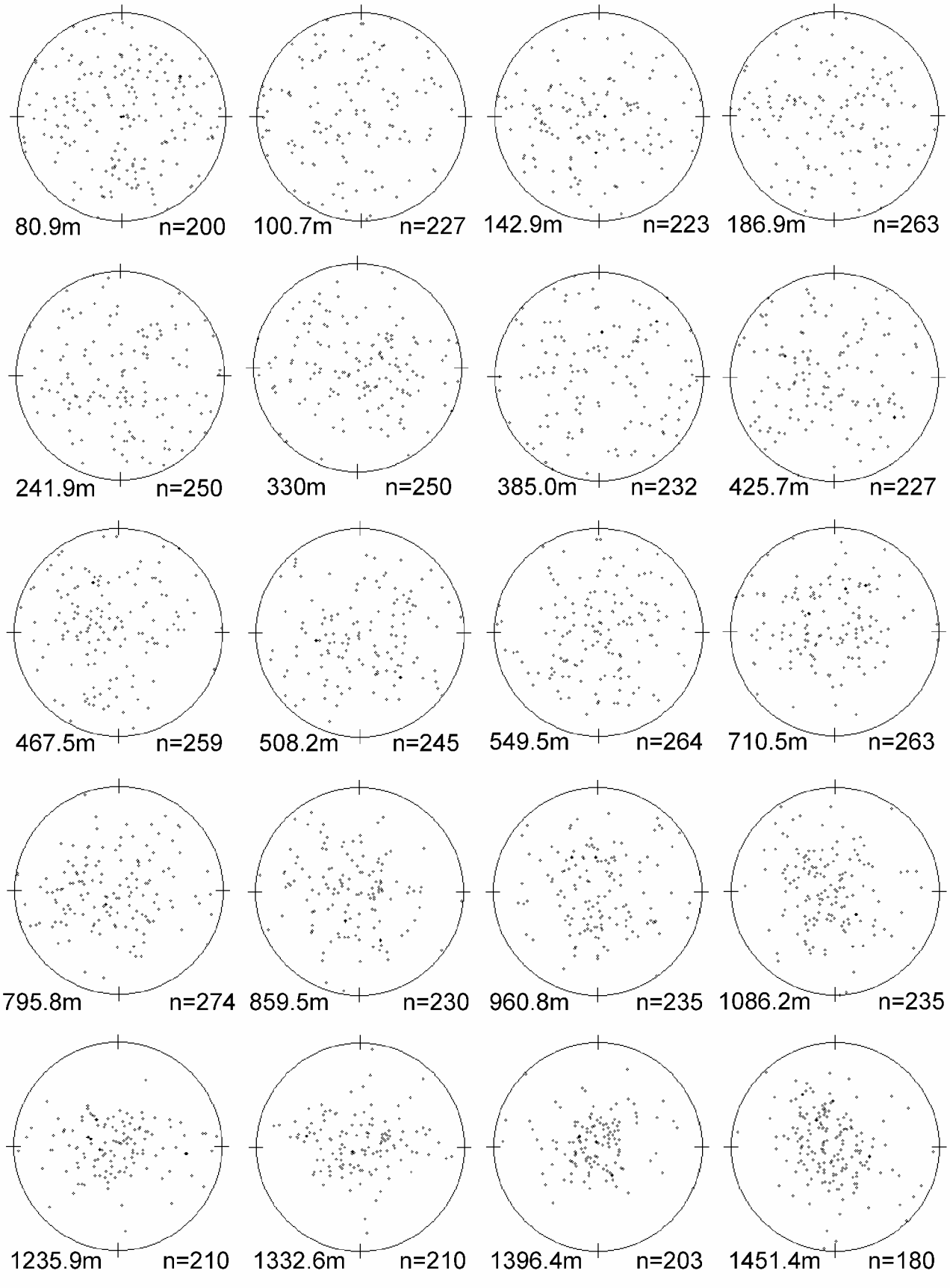

Fig. 1. Fabric diagrams. The number of measured c axes and the depth are indicated below each diagram. A line passing through the centre of each diagram corresponds to the core axis.

urements were carried out at the Alfred Wegener Institute in 2000 and 2001, and some samples were remeasured in 2002.

The measurements of fabrics and textures in the Dome C ice core were performed with an AIFA previously used to study the fabric evolution in the NorthGRIP ice core (Wang and others, 2002). The method used to derive the *c*-axis orientations has been described in detail by Wang and Azuma (1999) and by Wang and others (2002). In addition to fabric measurements, the images taken of the thin sections placed between crossed polarizers, at several different rotation positions of the polarizers, are used to derive information on crystal sizes and shapes, using the functions of an image-processing software package

https://doi.org/10.3189/172756403781816031 Published online by Cambridge University Press

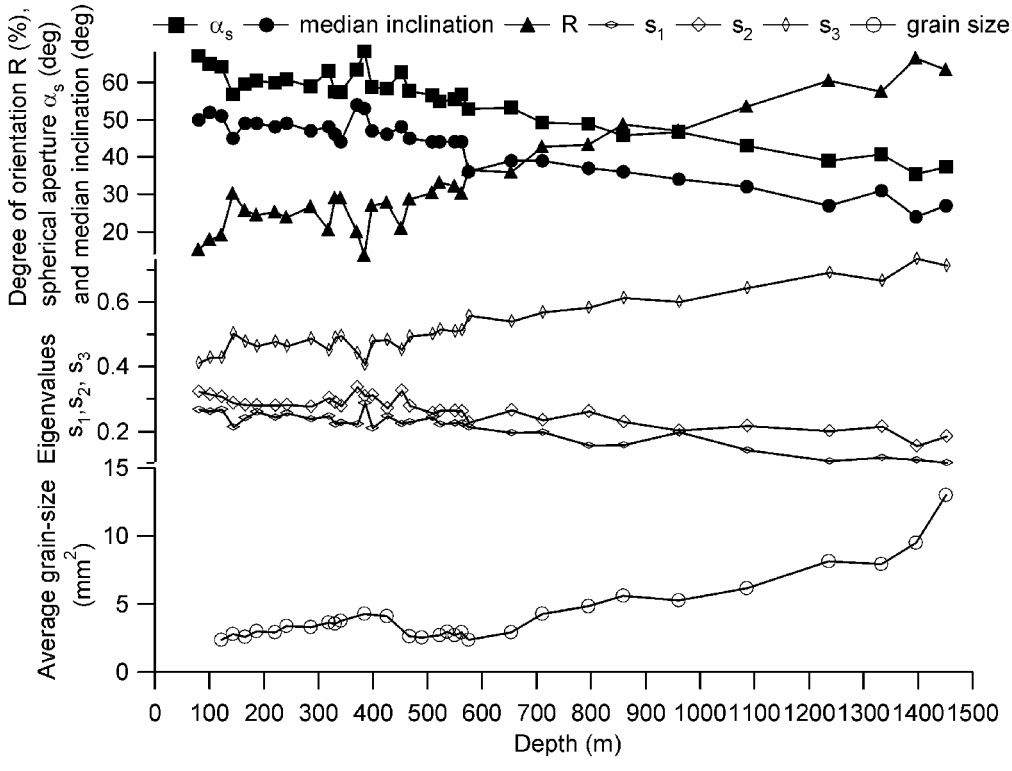

Fig. 2. Fabric statistics and crystal size. The degree of orientation (R) varies between 0% for a random fabric and 100% for completely parallel c axes. The spherical aperture (α_s) can be visualized in a similar way to the half-angle of a cone enclosing the c axes in a sample. The eigenvalues represent the lengths of eigenvectors along the axes of an ellipsoid that best fits the distribution of c axes. For definitions of these parameters see Wallbrecher (1979) and Thorsteinsson (1996). Median inclination and crystal size measurements are explained in the text.

(ImagePro). The method and procedure are described in Wang and Azuma (1999). For this study, additional software has been developed to determine the misorientation angles between the *c* axes of neighbouring ice crystals. Each pair of adjacent crystals in each dataset was used in this analysis. Following Alley and others (1995), the misorientation was then weighted by the misorientation between randomly selected pairs of crystals.

Independent of the fabric study, microscopic observations on thick sections from the Dome C core have been carried out on site. A method has been developed to map microstructural features such as grain boundaries, sub-grain boundaries, slip bands and air inclusions directly on the surface of thick sections or inside them. This method is briefly described below and will be presented in detail elsewhere. The observations were carried out in the field (austral season 2000/01), generally a few days after the cores were drilled. Samples were taken at 11 m intervals. The dimensions of a thick section were 4.5×9 cm with a thickness of 5 mm. Before freezing the sample on a glass plate, the microtomed surface was allowed to sublimate to erode grain and sub-grain boundary grooves and make them visible. Each thick section was mounted on a horizontal stage which can be moved in prescribed *X* and *Y* directions. At each *XY*-stage position, images were taken by a charge-coupled device (CCD) video camera attached to a microscope, and recorded digitally on a computer hard disk. During the mapping of grain and sub-grain boundaries, the microscope is focused on the upper surface of a thick section. Neighbouring images are slightly overlapping to allow the reconstruction of the grain-boundary network of the whole section. A series of about 1500 images is necessary to map the surface of a thick section. An image-acquisition system based on the NIH/SCION Image software running on a Macintosh computer is used to merge all images in order to obtain an image of the entire surface of a section.

RESULTS

Figure 1 presents the fabric diagrams resulting from the *c*-axis measurements on thin sections from the Dome C core. The results from 80.85 and 508.2 m are obtained directly from horizontal thin sections, but all other diagrams are obtained by rotating *c*-axis data obtained from vertical thin sections and then projecting them into the horizontal plane. The core axis is thus parallel to a line passing through the centre of the diagram. Following suggestions made at a recent workshop on the presentation of ice crystal data obtained with automatic fabric analyzers (University of Copenhagen, 2002), a fabric diagram size of 4×4 cm was used and 200 *c*-axis orientations were randomly selected from the measured ones and plotted in each fabric diagram. Each point represents the projection of a *c* axis on an equal-area diagram. It can be seen that the projections of the *c* axes are distributed quasi-randomly at shallow depths. The *c* axes gradually become clustered around the centre with increasing depth and finally form a broad single maximum. Statistical analysis of the data, presented in Figure 2, confirms this tendency. To describe the evolution of fabric strength and shape, we use the *degree of orientation* (*R*), the *spherical aperture* (α), the *median c-axis inclination* and three *eigenvalues* (see definitions in Wallbrecher, 1979; Thorsteinsson, 1996). These parameters have previously been used to describe *c*-axis orientations in the GRIP (Thorsteinsson and others, 1997) and NorthGRIP ice cores (Wang and others,

https://doi.org/10.3189/172756403781816031 Published online by Cambridge University Press

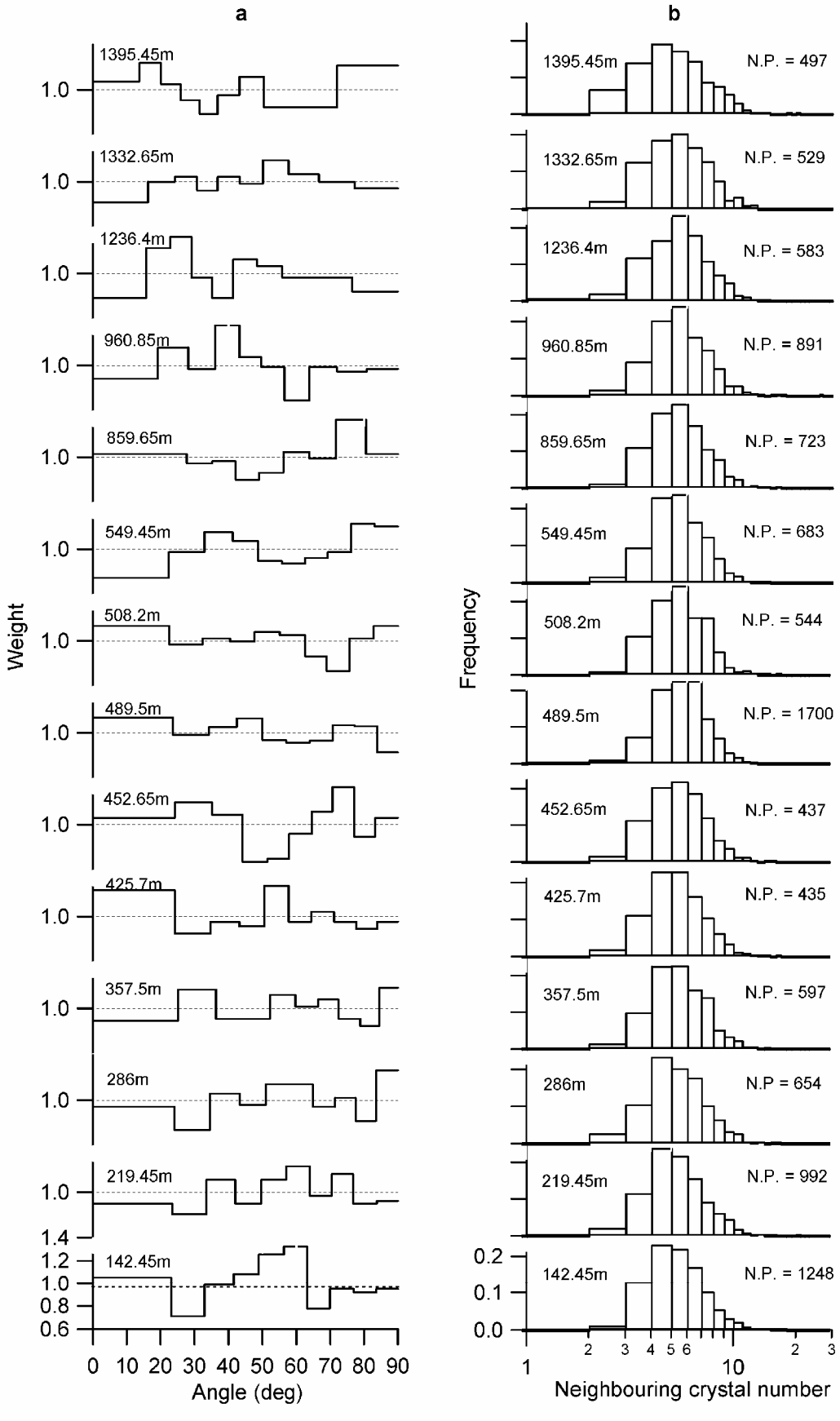

Fig. 3. Results from the study of misorientation angles: (a) weighted misorientation angles of neighbouring crystals; (b) histograms of the number of neighbouring crystals. On the right side of each histogram, N.P. gives the number of pairs of neighbouring crystals, including crystals whose c-axis orientations were not measured.

2002). R and α are measures of fabric strength, whereas eigenvalues can be used to characterize the shape of the c-axis orientation distribution. Median inclination (introduced by Russell-Head and Budd, 1979) is defined as the half-angle of a solid cone distribution in which 50% of c axes are included. Like R and α, this parameter is mainly useful for describing the evolution towards a single-maximum fabric. From Figure 2 it is evident that the strength of the Dome C fabric increases

https://doi.org/10.3189/172756403781816031 Published online by Cambridge University Press

Table 1. Depths and orientations of thin sections used for the study of misorientation angles. The number of measured c axes and number of pairs of neighbouring crystals are indicated

Depth m	*H(orizontal) or V(ertical) cutting*	*Measured c axes*	*Pairs of neighbouring crystals*
142.45	V	223	295
219.45	V	249	434
286.00	V	255	501
357.50	V	235	484
425.70	V	227	482
452.65	H	215	370
489.50	V	553	1195
508.20	H	245	349
549.45	V	264	402
859.65	V	230	498
960.85	V	235	477
1236.40	V	210	510
1332.65	V	210	500
1395.45	V	203	496

steadily with depth, as can be seen from the increase of R and the decrease of α and median inclination. The normalized eigenvalues s_1, s_2 and s_3 calculated for each diagram show that s_3 slowly becomes larger than s_1 and s_2, which is consistent with a slight concentration of the c axes around the vertical with increasing depth. Figure 2 also presents results from measurements of mean crystal areas, which were measured from thin-section images using the ImagePro software.

The results of the analysis of misorientation angles between the c-axis orientations of neighbouring crystals are shown in Figure 3. In Figure 3a, a weight <1 indicates a shortage of pairs of neighbouring crystals within a range of misorientation, and weights >1 indicate an excess of pairs of neighbours in that range. The number of pairs of neighbouring crystals deduced from c-axis orientation measurements on selected samples is shown in Table 1. Histograms of the number of neighbouring crystals for all crystals of the same sections are shown in Figure 3b.

Two typical examples of microscopic observations of sub-grain boundaries are shown in Figures 4 and 5. In each image a series of arrows marks the sub-boundaries. We assume that Figure 4 illustrates sub-boundaries at an early stage, while Figure 5 shows a sub-boundary at a late stage. In the early stage of the formation of sub-grain boundaries the misorientation between the two sub-grains is low and can only be recognized as slightly differing grey values under a polarizing microscope at high magnification. Summarizing our preliminary observations on thousands of images, it seems that at the early stage of sub-boundary formation, sub-boundaries are characterized by an irregular structure and cluster at limited parts of a grain. By contrast, a sub-grain boundary in the fully developed stage appears as a smooth or even straight line (Fig. 5). Occasionally slip bands are observed that allow us to determine the misorientation of basal planes between the sub-grains directly in the image.

DISCUSSION

Data on crystal size variations in the uppermost 580 m of the Dome C core have been presented and discussed by Gay and Weiss (1999) and by Arnaud and others (2000). Image-analysis techniques were used to obtain these data. In contrast, crystal sizes in the old Dome C core drilled to 905 m

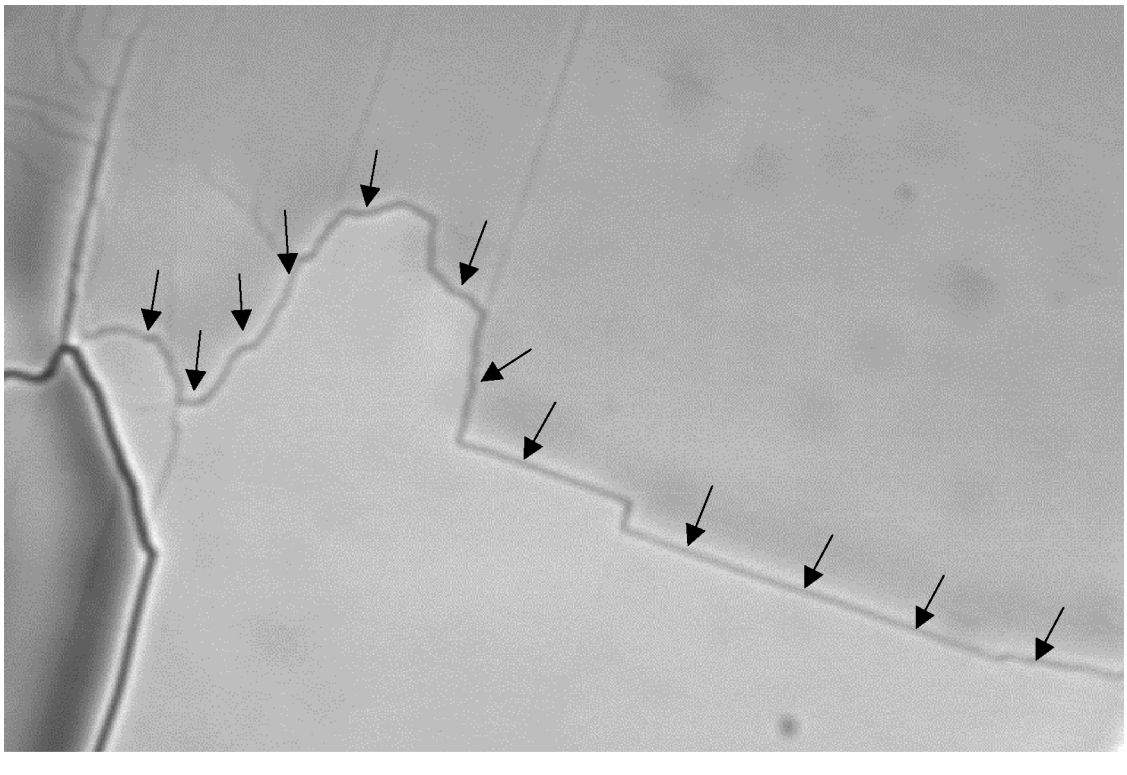

Fig. 4. Microscopic image of an ice thick section showing a sub-grain boundary, probably at an early stage of formation (sample from the depth interval 150–299 m; exact depth unknown). The black arrows mark the position of the sub-boundary. The image is taken between crossed polarizers. The difference in greyness across the sub-boundary indicates slightly different orientation of the c axis in the two parts of the grain.

https://doi.org/10.3189/172756403781816031 Published online by Cambridge University Press

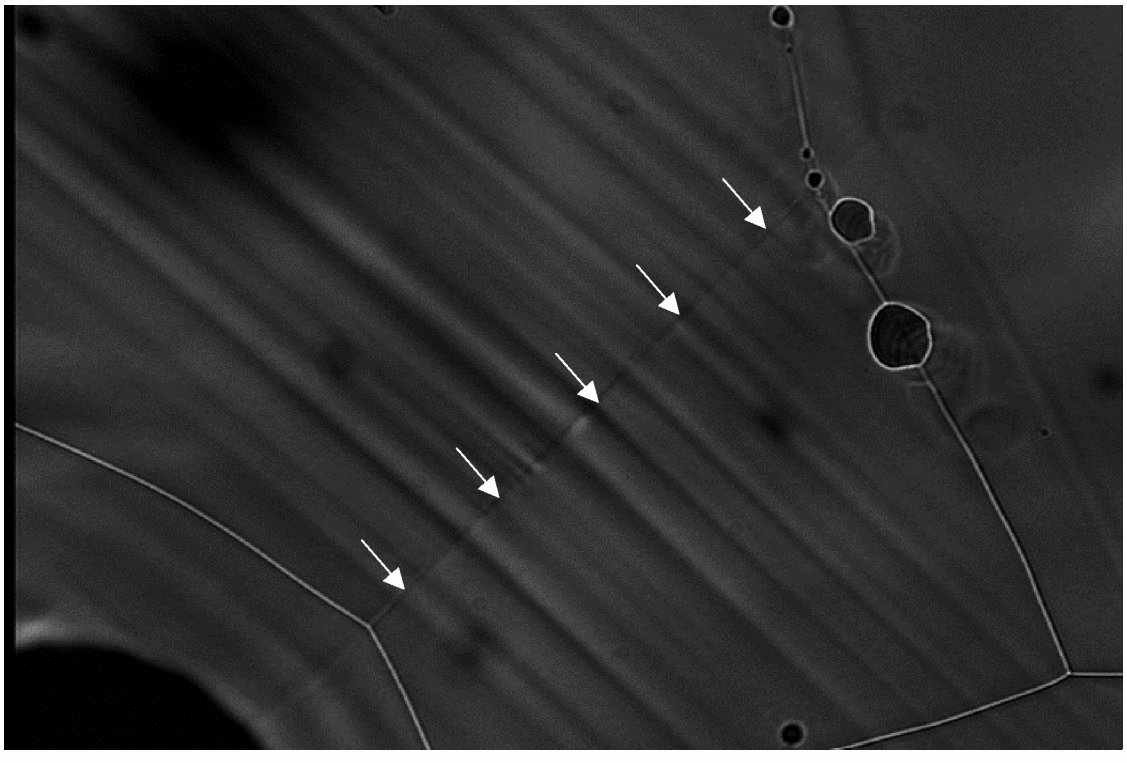

Fig. 5. Microscopic image of an ice thick section with a sub-grain boundary at a late stage of formation (depth: 611 m). The white arrows mark the position of the sub-boundary. The difference in orientation of the slip bands in the sub-grains indicates a misorientation of basal planes (and hence c axes) of a few degrees. The near-circular features located on the grain boundary to the right are air bubbles.

depth in 1979 (Duval and Lorius, 1980; Petit and others, 1987) were determined using older methods (Paterson, 1994). In accordance with the earlier results, the crystal areas presented in Figure 2 show a trend towards larger crystal sizes in the uppermost 420 m, due to normal grain growth in ice dating from the Holocene. Crystal sizes decrease below 420 m, as the Wisconsinan ice is entered, but continue to increase below 600 m. The overall development appears similar to crystal size variations at other sites in East Antarctica, such as Vostok (Lipenkov and others, 1989) and Dome F (Azuma and others, 1999). Although the general trends in both datasets are very similar, the crystal areas presented here are consistently larger than the results obtained by Arnaud and others (2000). This must be due to the different methods used to estimate crystal areas from thin-section images. There is an obvious need to standardize measurements of crystal sizes that rely on image-analysis techniques.

In Figure 6, the median inclination (MI) of the *c*-axis distribution in the Dome C core is compared with median inclinations in the GRIP (Thorsteinsson and others, 1997) and Dome F (Azuma and others, 1999) ice cores. The variations of MI in the three cores are plotted against the normalized depth (i.e. depth/ice thickness). Assuming steady-state conditions and a uniform strain rate through the ice following a simple model (Nye model), the cumulative strain can be assumed to be approximately equal at the same normalized depth at all three locations. The results of a *c*-axis rotation model (Azuma, 1994; solid line in Fig. 6) are compared with the observations. The three datasets are in good agreement, supporting previous assumptions that fabric strength in the upper 80% of the thickness of polar ice sheets mainly depends on the cumulative strain and is largely independent of impurities, accumulation rate and temperature.

The purpose of studying the *c*-axis orientations of neighbouring crystals is to investigate the different processes involved in texture development, such as the impeding effect of dust particles on grain-boundary migration (boundary pinning), polygonization due to dislocation pile-up to form sub-boundaries in a crystal, and recrystallization involving the nucleation of new strain-free crystals. According to Alley and others (1995, fig. 4), the misorientation angle between the *c* axes of neighbouring crystals should be random for isotropic ice at the surface of ice sheets, and the weight at every range of misorientation angles should be 1. If boundary pinning dominates, the weight should not change and all values should be close to 1. If recrystallization is dominant, nucleation of grains with *c* axes at high angles to their neighbours could be expected to occur; thus the weight at high angles should be larger than 1 and increase with depth. In contrast,

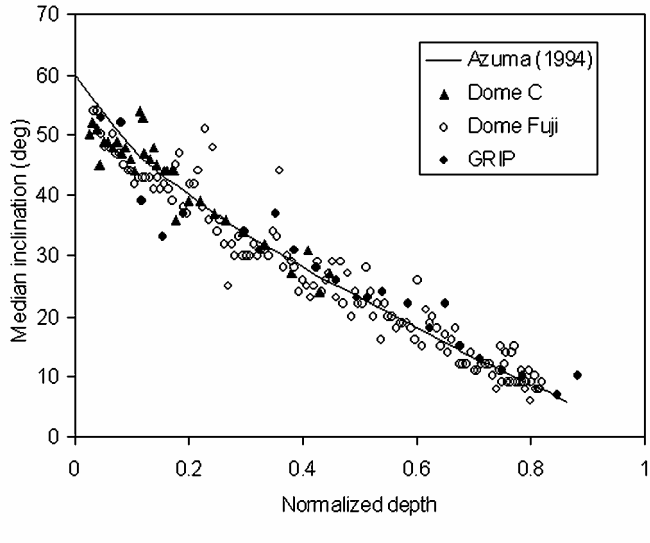

Fig. 6. Median inclination of the c-axis distribution against normalized depth (depth/ice thickness) at Dome C, Dome F, GRIP and Azuma's (1994) model.

https://doi.org/10.3189/172756403781816031 Published online by Cambridge University Press

if polygonization is dominant, a surplus of low angles can be expected since a pre-existing crystal splits into two or more new crystals with similar orientations. Consequently, the weight at low angles will be larger than 1 and increase with depth. In Figure 3, down to 425 m the weights at all the angles are close to 1 and the weight at angles exceeding 60° is slightly higher. At 425–522 m depth, the weight at low angles (<20°) is higher than 1. At 522–1236 m depth, there is no clear tendency. This could at first sight be interpreted as evidence for polygonization in the interval 425–522 m. The observed crystal-size decrease in this depth interval could then be interpreted as additional evidence for polygonization, since this recrystallization process can lead to a decrease in average crystal size. We believe, however, that the decrease in crystal size is mainly due to the effect of soluble and insoluble impurities on grain-boundary migration (Weiss and others, 2002), and the available evidence from the neighbouring crystal study seems too weak to conclude that polygonization is active in this interval.

Microscopic observations on fresh ice-core samples at the drilling site indicate that about half of all grains in the depth interval 150–1300 m contain sub-grain boundaries. If all of these sub-boundaries can develop to reach the late stage as shown in Figure 5, with a misorientation of a few degrees, the weight of low angles will always be high and reach a value of 4. Such a high value was, however, obtained neither in this study nor in the misorientation study of Alley and others (1995). The reason could be that not all the observed sub-boundaries grow into a normal grain boundary with a misorientation angle greater than several degrees. It is likely that some sub-boundaries near an old grain are consumed by the migration of the boundary of the old grain. Another reason could be that the sub-boundaries are weak and hard to detect with the naked eye or the CCD camera of our current automatic fabric analyzer. It is difficult or even impossible to recognize crystals splitting up into two or more crystals. We suppose that Alley and others (1995) had the same problem identifying split grains since they used a Rigsby stage to measure *c*-axes orientation. To circumvent these problems, it would be necessary to investigate the misorientations between sub-grains on the microscopic scale with higher resolution and study how many already-formed sub-boundaries lead to the subdivision of grains.

The number of neighbouring crystals shown in Figure 3b displays a log-normal distribution. On average, each grain has 5.4–5.6 neighbours at all depths. According to Atkinson (1988), the perfect two-dimensional crystal in equilibrium has six sides and is surrounded by six neighbours. Such equilibrium is never present in glacial ice, and, on average, crystals with more than six sides will grow and crystals with less than six sides will shrink. We find that the number of crystals with less than six neighbours is about twice as high as the number with more than six neighbours. Hence it can be deduced that the average value of about 5.5 neighbours per crystal indicates that about two-thirds of all grains are smaller than the average grain-size and thus shrink to compensate for the growth of the bigger grains.

CONCLUSIONS

Ice fabric analysis of the Dome C core down to 1500 m depth shows that a quasi-random fabric at the surface evolves toward a broad single-maximum fabric with increasing depth. This suggests that at Dome C the ice is subject mainly to vertical uniaxial compression. Comparison with the Dome F and GRIP ice cores where the same kind of stress system governs ice deformation provides additional support for the assumption that basal glide is the dominating mechanism for fabric development at low temperatures in the upper parts of polar ice sheets. Fabric strength in the depth interval being considered here mainly depends on the cumulative strain, and is independent of impurity content, accumulation rate and temperature. Preliminary results from crystal size measurements indicate a development of crystal size at Dome C similar to that in the Vostok and Dome F deep cores.

Results from a study of misorientation angles between the *c* axes of neigbouring grains, using the method of Alley and others (1995), indicate that recrystallization involving the nucleation and growth of new grains at high angles to the axis of compression is not active in the upper 1500 m of the Dome C core. The study does not reveal conclusive evidence on the possible occurrence of polygonization. However, microscopic observations show that sub-grain boundaries are present in about half of all crystals in the depth interval 150–1300 m. There are likely two reasons for the conflict arising here: (1) Not all the sub-boundaries can develop enough to split the original crystals, and they are consumed by the migration of old grains; and (2) the resolution of current *c*-axis orientation measurements is not high enough to identify these sub-grains. Fabric investigations on a microscopic scale should be carried out in future studies.

ACKNOWLEDGEMENTS

This work is a contribution to the "European Project for Ice Coring in Antarctica" (EPICA), a joint European Science Foundation/European Commission (EC) scientific program, funded by the EC under the Environment and Climate Program and by national contributions from Belgium, Denmark, France, Germany, Italy, the Netherlands, Norway, Sweden, Switzerland and the United Kingdom. Th. Thorsteinsson thanks the Icelandic Research Council (RannIs) for support.

REFERENCES

Alley, R. B. 1988. Fabrics in polar ice sheets: development and prediction. *Science*, **240**(4851), 493–495.

Alley, R. B. 1992. Flow-law hypotheses for ice-sheet modeling. *J. Glaciol.*, **38**(129), 245–256.

Alley, R. B., A. J. Gow and D. A. Meese. 1995. Mapping *c*-axis fabrics to study physical processes in ice. *J. Glaciol.*, **41**(137), 197–203.

Arnaud, L., J. Weiss, M. Gay and P. Duval. 2000. Shallow-ice microstructure at Dome Concordia, Antarctica. *Ann. Glaciol.*, **30**, 8–12.

Atkinson, H.V. 1988. Theories of normal grain growth in pure single phase systems. *Acta Metall.*, **36**(3), 469–491.

Azuma, N. 1994. A flow law for anisotropic ice and its application to ice sheets. *Earth Planet. Sci. Lett.*, **128**(3–4), 601–614.

Azuma, N. and A. Higashi. 1985. Formation processes of ice fabric pattern in ice sheets. *Ann. Glaciol.*, **6**, 130–134.

Azuma, N. *and 6 others*. 1999. Textures and fabrics in the Dome F (Antarctica) ice core. *Ann. Glaciol.*, **29**, 163–168.

Duval, P. and C. Lorius. 1980. Crystal size and climatic record down to the last ice age from Antarctic ice. *Earth Planet. Sci. Lett.*, **48**(1), 59–64.

Fujita, S., M. Nakawo and S. Mae. 1987. Orientation of the 700-m Mizuho core and its strain history. *Proc. NIPR Symp. Polar Meteorol. Glaciol.* 1, 122–131.

Gay, M. and J. Weiss. 1999. Automatic reconstruction of polycrystalline ice microstructure from image analysis: application to the EPICA ice core at Dome Concordia, Antarctica. *J. Glaciol.*, **45**(151), 547–554.

Jacka, T. H. and M. Maccagnan. 1984. Ice crystallographic and strain rate changes with strain in compression and extension. *Cold Reg. Sci. Technol.*, **8**(3), 269–286.

Lipenkov, V. Ya., N. I. Barkov, P. Duval and P. Pimienta. 1989. Crystalline texture of the 2083 m ice core at Vostok Station, Antarctica. *J. Glaciol.*, **35**(121), 392–398.

Paterson, W. S. B. 1994. *The physics of glaciers. Third edition*. Oxford, etc., Elsevier.

Petit, J. R., P. Duval and C. Lorius. 1987. Long-term climatic changes indicated by crystal growth in polar ice. *Nature*, **326**(6108), 62–64.

Pimienta, P., P. Duval and V. Ya. Lipenkov. 1987. Mechanical behavior of anisotropic polar ice. *International Association of Hydrological Sciences Publication* 170 (Symposium at Vancouver 1987 — *The Physical Basis of Ice Sheet Modelling*), 57–66.

Russell-Head, D. S. and W. F. Budd. 1979. Ice-sheet flow properties derived from bore-hole shear measurements combined with ice-core studies. *J. Glaciol.*, **24**(90), 117–130.

Shoji, H. and C. C. Langway, Jr. 1988. Flow-law parameters of the Dye 3, Greenland, deep ice core. *Ann. Glaciol.*, **10**, 146–150.

Thorsteinsson, Th. 1996. Textures and fabrics in the GRIP ice core, in relation to climate history and ice deformation. *Ber. Polarforsch.* 205.

Thorsteinsson, Th., J. Kipfstuhl and H. Miller. 1997. Textures and fabrics in the GRIP ice core. *J. Geophys. Res.*, **102**(C12), 26,583–26,599.

Wallbrecher, E. 1979. Methoden zum quantitativen Vergleich von Regelungsgraden und -formen strukturgeologischer Datenmengen mit Hilfe von Vektorstatistik und Eigenwertanalyse. *Neues Jahrb. Geol. Paläontol.* 159, 113–149.

Wang Yun and N. Azuma. 1999. A new automatic ice-fabric analyzer which uses image-analysis techniques. *Ann. Glaciol.*, **29**, 155–162.

Wang, Y., Th. Thorsteinsson, J. Kipfstuhl, H. Miller, D. Dahl-Jensen and H. Shoji. 2002. A vertical girdle fabric in the NorthGRIP deep ice core, North Greenland. *Ann. Glaciol.*, **35**, 515–520.

Weiss, J., J. Vidot, M. Gay, L. Arnaud, P. Duval and J. R. Petit. 2002. Dome Concordia ice microstructure: impurities effect on grain growth. *Ann. Glaciol.*, **35**, 155–162.

https://doi.org/10.3189/172756403781816031 Published online by Cambridge University Press